Chinese Chemical Letters 31 (2020) 521–524

Contents lists available at ScienceDirect

Chinese Chemical Letters

journal homepage: www.elsevier.com/locate/cclet

Communication

Two-dimensional mesoporous sensing materials

Yu Wen[a], Facai Wei[a], Wenqian Zhang[a], Anyang Cui[b], Jing Cui[a], Chengbin Jing[a], Zhigao Hu[b], Qingguo He[c], Jianwei Fu[d], Shaohua Liu[a,c,*], Jiangong Cheng[c,**]

[a] State Key Laboratory of Precision Spectroscopy & School of Physics and Materials Science, East China Normal University, Shanghai 200241, China
[b] Key Laboratory of Polar Materials and Devices (MOE) and Technical Center for Multifunctional Magneto-Optical Spectroscopy (Shanghai), Department of Electronic Engineering, East China Normal University, Shanghai 200241, China
[c] State Key Lab of Transducer Technology, Shanghai Institute of Microsystem and Information Technology, Chinese Academy of Sciences, Shanghai 200050, China
[d] School of Materials Science and Engineering, Zhengzhou University, Zhengzhou 450052, China

ARTICLE INFO

Article history:
Received 25 March 2019
Received in revised form 26 April 2019
Accepted 29 April 2019
Available online 30 April 2019

Keywords:
Two-dimensional materials
Mesoporous polymer
Polypyrrole
Chemical sensing
Self-assembly

ABSTRACT

Two-dimensional mesoporous materials combing ultrathin nanosheet morphology with well-defined mesoporous structures, are now emerging and becoming increasingly important for their promising applications in energy storage, electronic devices, electrocatalysts and so on. Here, we synthesized a kind of polypyrrole-based two-dimensional mesoporous materials with uniform pore size, ultrathin thickness and high surface area. Serving for electrochemical NH_3 sensor, they exhibited a fast response and high sensitivity. Therefore, our study would promote much interest in design of new materials for gas sensor applications.

Owing to the unique two-dimensional (2D) morphology, ultrathin thickness and high surface area, 2D materials have been intensively researched in recent years, which present the tremendous potential for diverse applications, such as chemical gas sensors, energy storage, electronic devices, electrocatalysts [1–8]. Besides, 2D materials can provide multiple active sites, high flexibility and good processability, which are particularly important for construction of high-performance gas sensors [9]. For example, graphene has been exploited as sensor to detect single NO_2 gas molecule at room temperature, exhibiting an ultrahigh sensitivity [10]. Addtionally, the working temperature of gas sensors can even decrease to room temperature for the participation of some 2D materials, which greatly facilitated their practical application [11–13].

Mesoporous materials with uniform pore size (2–50 nm), high surface area, large pore volume and modifiable surface, have been widely employed as supports for catalysis, separation, selective adsorption, even as hosts to include guest molecules over the past few years. Creating abundant mesopores along in-plane direction in nanosheets, can provide for 2D materials with higher surface area and additional active sites, thereby rendering them with enhanced electrochemical storage capacity, catalytic activity and filtration capability [14–26]. For the most of gas sensors, the sensing mechanisms are depended on the interaction of gas molecules with the surface of solid materials, therefore, it is highly desired to develop 2D mesoporous materials for gas sensing with defined porous structure, large surface area and well-defined surface properties [27–32]. However, up to now, exploring 2D mesoporous materials for gas sensor still remains unresolved, maybe due to the lack of suitable materials [33].

Here, we synthesized 2D mesoporous polypyrrole (2D mPPy) nanosheets with hierarchical nanopores (mesopores of about 18 nm and micropores of about 1 nm) *via* a soft-template directing co-assembly route. The resultant materials featured uniform pore size, ultrathin thickness and high surface area. Serving as electrochemical sensor, the 2D mPPy nanosheets exhibited a fast response and high sensitivity for ammonia gas (NH_3). As known, NH_3 is widely used in manufacturing and agricultural production, but, as a highly toxic gas, it can irritate the skin, eyes and respiratory tract, and cause lung disease by reacting with the other air pollutants (nitrogen or sulfur) to form particles smaller than 2.5 μm (PM2.5) [34,35]. Therefore, it was expected that 2D mPPy would offer a new choice for the high-performance NH_3 sensor.

* Corresponding author at: State Key Laboratory of Precision Spectroscopy & School of Physics and Materials Science, East China Normal University, Shanghai 200241, China.
** Corresponding author.
E-mail addresses: shliu@phy.ecnu.edu.cn (S. Liu), jgcheng@mail.sim.ac.cn (J. Cheng).

https://doi.org/10.1016/j.cclet.2019.04.071
1001-8417/

The previous study demonstrated that amphiphilic surfactants of perfluorinated carboxylic acid (PFCA) can self-assemble into bilayer-structured micelles in a mixed solvent of EtOH/H_2O, which can serve as an exquisite whilst robust platform for the guest moieties to be self-assembled on both of their surfaces [36]. Compared with the common surfactants (such as aliphatic amine, *etc.*), PFCA possesses smaller surface energy and could form more stable assembling structures. In addition, the abundant carboxyl functional groups of PFCA bilayers would be more favorable to guide the polymerization of pyrrole monomers, because of the electrostatic interaction between carboxyl groups of PFCA and imino groups of pyrroles [36,37]. On the other hand, PS-*b*-PEO block co-polymer (BCP) can self-assemble into spherical micelles in a mixed solvent of THF/H_2O at room temperature, rearranging into close-packed monolayers around the surfaces of PFCA bilayer through H-bonding between the PEO chains and PFCA. Subsequently, after adding pyrrole monomers and ammonium persulfate (APS), the above hierarchical supermolecule assemblies of BCP@PFCA can guide the polymerization of pyrrole monomers under triggering of APS. Upon the complete removal of the BCP and PFCA templates, the 2D mPPy nanosheets were obtained. The above mechanism is similar to the growth of PPy directed by aliphatic amine, but here an improved method was adopted, and the detailed experimental procedure can be seen from Supporting information.

We performed a serial of characterizations to testify the synthesized 2D mPPy nanosheets. As seen from the Fourier-transform infrared (FT-IR) spectra (Fig. S1 in Supporting information), the obtained 2D mPPy nanosheets showed the typical symmetric stretching vibration of the pyrrole rings at 1541 cm^{-1} and 1458 cm^{-1}, and asymmetric stretching vibration of the pyrrole rings at 1277 cm^{-1} and 1024 cm^{-1}, as well as stretching vibration of =C—N and twisting vibration of =C—H of polymeric pyrrole, indicating the formation of PPy [38–40]. Moreover, the synthesized 2D mPPy nanosheets and the control samples (noted as PPy-blank, synthesized without any templates) exhibited the almost same infrared signals in the wavenumber range of 500-4000 cm^{-1}, which can prove the complete removal of BCP and PFCA templates. Moreover, the characteristic peaks of BCP and PFCA, including Ar-H, —CH_2/—CH_3, C=C of aromatic benzene rings, and carboxyl and alkyl signals of PFCA, cannot be found in the IR spectra of the 2D mPPy nanosheets, which also versified the removal of templates.

The UV–vis spectroscopy showed that the 2D mPPy nanosheets possessed the similar signals with the PPy-blank materials (Fig. S2 in Supporting information). Among them, the signal of ~330 nm corresponds to the π–π^* electronic transition of pyrrole ring, while the signal of ~420 nm is attributed to the polarization peak of PPy [41,42].

The morphology of the obtained PPy can be observed by the scanning electron microscopy (SEM, Fig. 1), which revealed that the resultant PPy samples possessed 2D ultrathin nanosheet architecture, and uniformly distributed mesopores with pore diameter of approximately 15–20 nm. In contrast, we only obtained the irregular PPy nanoparticles if without any templates (PPy-blank), as shown Fig. S2. This result indicated that BCP and PFCA templates play a very important role in the synthesis of mPPy materials with unique morphology and structure.

The results of atomic force microscopy (AFM, Fig. 1b) also revealed that the prepared 2D mPPy nanosheets had a smooth surface with a total thickness of about 24 nm. As previously reported, the diameter of PS_{90}-*b*-PEO_{114} spherical micelles here used is about 12–15 nm [37]. Therefore, the thickness of the 2D mPPy nanosheets corresponds to the height of the two layers of BCP spherical micelles, indicating that the spherical BCP micelles would close pack on the both surfaces of PFCA into sandwich structure. In addition, some smaller PPy nanosheets can be also found in AFM images, which may be caused by the constant stirring, polymerization and removal of the template during the preparation of PPy.

Transmission electron microscopy characterization (Fig. 2) further demonstrated that 2D mPPy nanosheets obtained by this soft template-oriented strategy possessed uniform mesopores with a pore size of approximately 18 nm, consistent with the above SEM results. At the same time, the high-resolution TEM (HRTEM) also revealed the overlap of mesopores in vertical, which may be formed by the packing of different PPy layers. Therefore, we speculated that the formation of bilayer-structured PPy nanosheets may result from the simultaneous absorption, assembly and growth of PPy on the both of surfaces of PFCA bilayer templates. Interestingly, besides mesopores, some micropores of about 1 nm can be also found in the 2D mPPy nanosheets (Fig. 2d), may owing to the contribution of PEO chains by spreading and occupying space in PPy frameworks, their removal would lead to the formation of micropores. The Nitrogen adsorption analysis below would provide more evidences for the presence of micropores.

Powder X-ray diffraction (XRD, Fig. S3 in Supporting information) displayed a weak peak of 23.8° (2θ), corresponding to the π-π interaction of the aromatic ring between the PPy chains [39,40]. It indicated that the resultant materials consisted primarily of amorphous polymeric frameworks.

Nitrogen adsorption test manifested (Fig. 3) that the 2D mPPy nanosheets had uniform mesopore with a pore size of about 18 nm. This result is agreed to the above SEM and TEM characterizations. As shown in nitrogen adsorption analysis, besides mesopores, the 2D PPy nanosheets have some micropores and macropores. The mesopores are derived from the removal of BCP templates and the macropores may be made from the stacked ultrathin PPy nanosheets, while the micropores may be attributed to the occupation of the PEO chains in the PPy polymer frameworks, because the

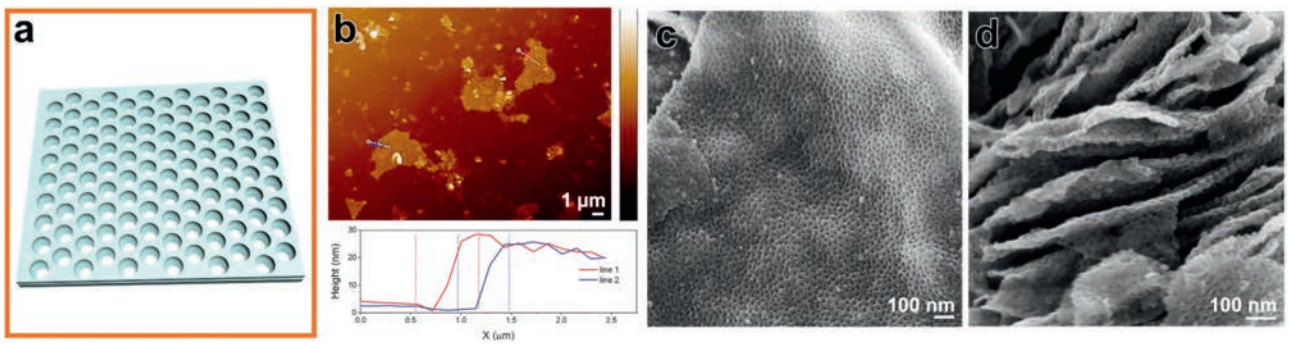

Fig. 1. Morphology and structure of the 2D mPPy nanosheets. (a) Schematic illustration of the 2D mPPy nanosheets. (b) AFM survey of the 2D mPPy nanosheets (Vertical scale: 114.2 nm). (c, d) SEM images of the 2D mPPy nanosheets.

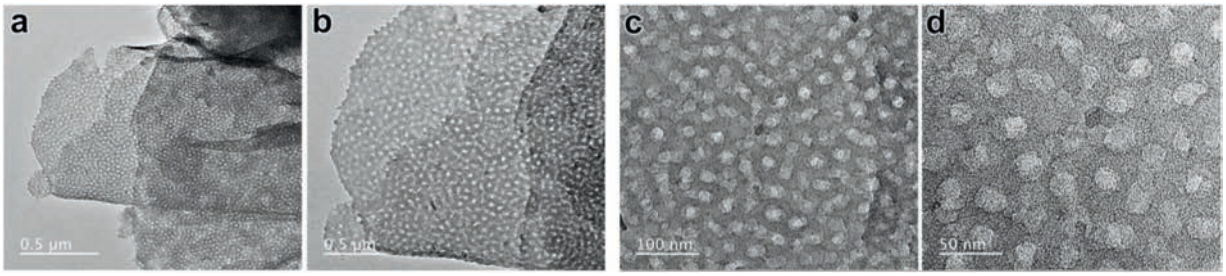

Fig. 2. TEM images of the 2D mPPy nanosheets at different magnifications.

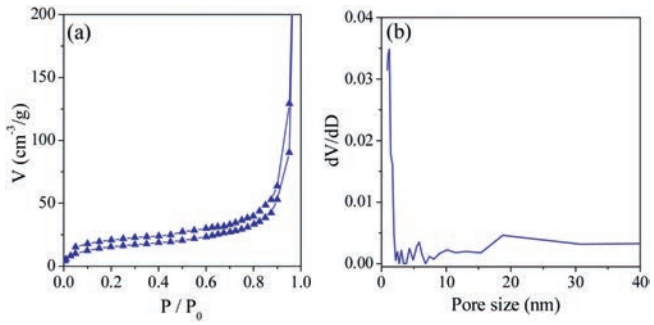

Fig. 3. Nitrogen adsorption–desorption isotherm and pore size distributions of the 2D mPPy nanosheets.

interaction of the PEO chains and the pyrrole monomers would lead to the assembly and growth of pyrrole around the PEO chains, then the PEO chains interspersed into the PPy polymer networks and generated microporous channels after BCP removal. Similar phenomena were often found in mesoporous silica and carbon systems [43–45]. Additionally, the BET surface area and pore volume of the 2D mPPy nanosheets were 56 m^2/g and 0.64 cm^3/g, respectively, which were close to the previously reported 2D mesoporous PPy [37]. In contrast, the PPy-blank sample has a BET surface area of only 25 m^2/g. This result indicates that BCP and PFCA templates are of great importance to the formation of 2D mesoporous materials with high specific surface area.

Given their unique structure, including high specific surface area, regular mesoporous array and ultra-thin nanosheet structure, *etc.*, the 2D mPPy nanosheets would be a suitable candidate for gas sensing. Therefore, we further evaluated their sensing performance for NH_3 detecting.

The response and recovery properties of the 2D mPPy nanosheets for NH_3 are tested at 22 °C and relative humidity of 21%. Fig. 4a showed that the 2D mPPy nanosheets had an excellent sensitivity to NH_3, which can reach 42% even at very low concentration of 20 ppm. Further, the sensitivity increased with the increase of NH_3 concentration. The detecting limitation and sensitivity of the 2D mPPy nanosheets for NH_3 was very close to, or even exceeded those of the conventional PPy with the different morphologies of nanowires, nanotubes or films [46–50], although which are still needed to be improved. As a p-type conductor, the excellent conductivity of polypyrrole is mainly attributed to their hole migration. When NH_3 gas spread into polypyrrole frameworks, they can donate electrons to the holes of PPy and thus reduce the numbers of holes, resulting in an increase of the resistivity of PPy. The resistivity changes of PPy can be converted into the detectable signals for sensing device. Therefore, conducting polymer of PPy as a sensitive material can be used for NH_3 detecting [51]. Fig. 3 also demonstrated that, when escaping from NH_3, the resistance of the 2D mPPy nanosheets immediately dropped. The recovery time of resistance became gradually longer with the increase of cycle numbers, perhaps due to the inevitable entrapment of the residual NH_3 molecules in the mesoporous materials.

Furthermore, we compared the NH_3 sensing performance of the 2D mPPy nanosheets with PPy-blank samples. As shown in Fig. 4b, when the NH_3 concentration was 200 ppm, the 2D mPPy nanosheets exhibited a higher sensitivity than PPy-blank samples, because the higher specific surface area was favorable to the contact with gas molecules and thus improved their sensitivity. However, it would also result in a longer recovery time for the 2D mPPy nanosheets.

The sensing performance of the 2D mPPy nanosheets doped with different acids, such as hydrochloric acid (HCl) and p-toluenesulfonic acid (TsOH), were also investigated (Fig. 4c). At the same concentration (1 mol/L), the doping of HCl for the 2D mPPy nanosheets offered a higher sensitivity for NH_3 detecting, it may be because that HCl, as a smaller molecule, is relatively easier to dope into the compactly intertwined PPy chains.

We also investigated the response ability of the 2D mPPy nanosheets for different gases (200 ppm of NH_3, HCl, acetone

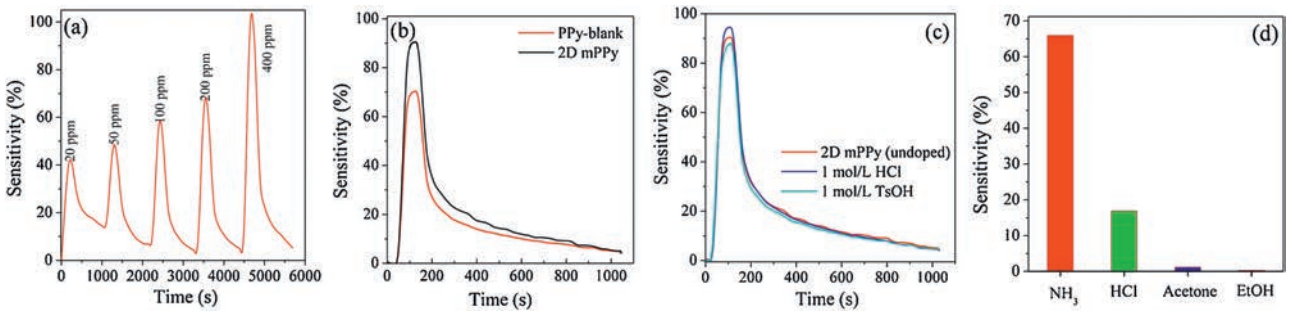

Fig. 4. The sensing performance of the 2D mPPy nanosheets. (a) The sensitivity of the 2D mPPy nanosheets for NH_3 with different concentrations. (b) The sensitivity of the 2D mPPy nanosheets and PPy-blank for NH_3 detecting. (c) The sensitivity for NH_3 detecting of the 2D mPPy nanosheets with different acids at 1 mol/L. (d) The detecting sensitivity of the 2D mPPy nanosheets for different gases.

and ethanol) (Fig. 4d). The results revealed the 2D mPPy nanosheets had the best response ability to NH_3, but a less response to HCl gas. Meanwhile, with regard to HCl detecting, they need longer response (119 s to 22 s) and recovery times (476 s to 173 s). In addition, the 2D mPPy nanosheets have almost no obvious response to acetone and ethanol. Compared to the other gases, such as HCl gas, acetone and EtOH, *etc.*, NH_3 possesses the stronger ability of giving electrons and are easier form NH_4^+, therefore, the device would have stronger adsorption and higher sensitivity for NH_3.

In conclusion, we synthesized the 2D mPPy nanosheets by a modified co-assembly strategy based on dual templates of PFCA and BCP, which featured a hierarchical nanopores (including mesopores and micropores), ultrathin thickness and high surface area. When serving for electrochemical sensor, the resultant 2D mPPy nanosheets exhibited a fast response and detection for NH_3. Therefore, we expect that this study would inspire more promising nanostructured materials for gas sensors.

Acknowledgment

This work was supported by the research programs from the National Natural Science Foundation of China (Nos. 51773062 and 61831021).

Appendix A. Supplementary data

Supplementary material related to this article can be found, in the online version, at doi:https://doi.org/10.1016/j.cclet.2019.04.071.

References

[1] F. Bonaccorso, L. Colombo, G. Yu, et al., Science 347 (2015) 1246501.
[2] M. Chhowalla, H.S. Shin, G. Eda, et al., Nat. Chem. 5 (2013) 263–275.
[3] Y. Guo, K. Xu, C. Wu, J. Zhao, Y. Xie, Chem. Soc. Rev. (2015) 637–646.
[4] Y. Shi, H. Li, L.J. Li, Chem. Soc. Rev. 44 (2015) 2744–2756.
[5] Z. Pei, H. Hu, G. Liang, C. Ye, Nano-micro Lett. 9 (2017) 19.
[6] M. Xu, T. Liang, M. Shi, H. Chen, Chem. Rev. 113 (2013) 3766–3798.
[7] X. Peng, L. Peng, C. Wu, Y. Xie, Chem. Soc. Rev. 43 (2014) 3303–3323.
[8] C. Chen, J. Xi, E. Zhou, et al., Nano-micro Lett. 10 (2018) 26.
[9] X. Liu, T. Ma, N. Pinna, J. Zhang, Adv. Funct. Mater. 27 (2017) 1702168.
[10] F. Schedin, A. Geim, S. Morozov, et al., Nat. Mater. 6 (2007) 652–665.
[11] P.A. Russo, N. Donato, S.G. Leonardi, et al., Angew. Chem. Int. Ed. 51 (2012) 11053–11057.
[12] S.Y. Cho, Y. Lee, H.J. Koh, et al., Adv. Mater. 28 (2016) 7020–7028.
[13] S. Cui, H. Pu, S.A. Wells, et al., Nat. Commun. 6 (2015) 8632.
[14] T. Lin, I.W. Chen, F. Liu, et al., Science 350 (2015) 1508–1513.
[15] Y. Xu, Z. Lin, X. Zhong, et al., Nat. Commun. 5 (2014) 4554.
[16] D. Zhou, Y. Cui, P.W. Xiao, et al., Nat. Commun. 5 (2014) 4716.
[17] K. Celebi, J. Buchheim, R.M. Wyss, et al., Science 344 (2014) 289–292.
[18] J. Liang, Y. Jiao, M. Jaroniec, S.Z. Qiao, Angew. Chem. Int. Ed. 51 (2012) 11496–11500.
[19] S.P. Koenig, L. Wang, J. Pellegrino, J.S. Bunch, Nat Nanotech. 7 (2012) 728–732.
[20] J. Bai, X. Zhong, S. Jiang, Y. Huang, X. Duan, Nat. Nanotech. 5 (2010) 190–194.
[21] Y. Fang, Y. Lv, J. Tang, et al., Angew. Chem. Int. Ed. 127 (2015) 8545–8549.
[22] D. Feng, Y. Lv, Z. Wu, et al., J. Am. Chem. Soc. 133 (2011) 15148–15156.
[23] J. Tang, J. Liu, C. Li, et al., Angew. Chem. Int. Ed. 54 (2015) 588–593.
[24] J. Liu, T. Yang, D.W. Wang, et al., Nat. Commun. 4 (2013) 2987.
[25] J. Liu, N.P. Wickramaratne, S.Z. Qiao, M. Jaroniec, Nat. Mater. 14 (2015) 763–774.
[26] Z. Cui, C. Zu, W. Zhou, A. Manthiram, J.B. Goodenough, Adv. Mater. (2016) 6926–6931.
[27] T. Wagner, S. Haffer, C. Weinberger, D. Klaus, M. Tiemann, Chem. Soc. Rev. 42 (2013) 4036–4053.
[28] Y. Li, W. Luo, N. Qin, et al., Angew. Chem. Int. Ed. 53 (2014) 9035–9040.
[29] J. Ma, Y. Ren, X. Zhou, et al., Adv. Funct. Mater. 28 (2018) 1705268.
[30] W. Luo, T. Zhao, Y. Li, et al., J. Am. Chem. Soc. 138 (2016) 12586–12595.
[31] G. Wang, J. Qin, X. Zhou, et al., Adv. Funct. Mater. 28 (2018) 1870364.
[32] Y. Zou, X. Zhou, Y. Zhu, et al., Acc. Chem. Res. 52 (2019) 714–725.
[33] Z. Wen, Q. Shen, X. Sun, Nano-micro Lett. 9 (2017) 45.
[34] E. Stokstad, Science 343 (2014) 238.
[35] X. Zhou, S. Lee, Z. Xu, J. Yoon, Chem. Rev. 115 (2015) 7944–8000.
[36] S. Liu, J. Zhang, R. Dong, et al., Angew. Chem. Int. Ed. 55 (2016) 12516–12521.
[37] S. Liu, F. Wang, R. Dong, et al., Adv. Mater. 28 (2016) 8365–8370.
[38] G. Cho, B.M. Fung, D.T. Glatzhofer, J.S. Lee, Y.G. Shul, Langmuir 17 (2001) 456–461.
[39] X. Zhang, J. Zhang, W. Song, Z. Liu, J. Phys. Chem. B 110 (2006) 1158–1165.
[40] Y. Ma, S. Jiang, G. Jian, et al., Energ. Environ. Sci. 2 (2009) 224–229.
[41] S.E. Mavundla, G.F. Malgas, D.E. Motaung, E.I. Iwuoha, J. Mater. Sci. 45 (2010) 3325–3330.
[42] C.T. Kuo, S.A. Chen, G.W. Hwang, H.H. Kuo, Synth. Met. 93 (1998) 155–160.
[43] M. Kruk, M. Jaroniec, C.H. Ko, R. Ryoo, Chem. Mater. 12 (2000) 1961–1968.
[44] M. Imperor-Clerc, P. Davidson, A. Davidson, J. Am. Chem. Soc. 122 (2000) 11925–11933.
[45] R. Ryoo, S.H. Joo, M. Kruk, M. Jaroniec, Adv. Mater. 13 (2001) 677–681.
[46] S.C. Hernandez, D. Chaudhuri, W. Chen, N.V. Myung, A. Mulchandani, Electroanalysis 19 (2007) 2125–2130.
[47] H. Yoon, M. Chang, J. Jang, J. Phys. Chem. B 110 (2006) 14074–14077.
[48] X. Yang, L. Li, Synth. Met. 160 (2010) 1365–1367.
[49] J.J. Lee, D. Yoo, C. Park, J.H. Kim, H.H. Choi, Macromol. Symp. 354 (2015) 280–286.
[50] H.J. Kharat, K.P. Kakde, P.A. Savale, et al., Polym. Adv. Technol. 18 (2007) 397–402.
[51] Y. Jiang, T. Wang, Z. Wu, et al., Sens. Actuators B -Chem. 66 (2000) 280–282.